2. RESULTS

2.1. Androgen-selective DNA response elements

2.1.1. Non-classical androgen response elements in the murine Pem promoter mediate selective transactivation

2.1.1.1. Selective stimulation of the Pem promoter by androgens

The murine *Pem* gene is a member of the *paired*-like class of homeobox genes. It is mainly expressed in the epididymis and ovary, but also in skeletal muscle and placenta. Its expression is strongly androgen-dependent in the testis and epididymis (Lindsey and Wilkinson, 1996; Sutton et al., 1996), but the molecular basis for this regulation is not known. It is also unclear if other steroids contribute to *Pem* transcription in the ovary or placenta.

In order to determine whether *Pem* was a direct AR target gene and to decipher the mechanisms governing its expression, two reporter plasmids containing parts of the murine *Pem* upstream region were devised. For the long construct, the region spanning from position –1139 to position -36 (Figure 8) was placed upstream of a luciferase reporter gene. For the short, proximal promoter construct, a fragment starting at position -444, just downstream of a muscle-specific exon and ending at position -36, was introduced into the same reporter vector.

CV-1 cells were used for transfection of the reporter plasmids as they do not express endogenous steroid receptors (Couette, et al., 1994; Szapary et al., 1996). The *Pem* promoter constructs were cotransfected together with expression vectors for the AR, GR or PR, and treated with the appropriate steroid (Figure 7). For both promoter constructs, the strongest stimulation was noted following AR cotransfection and R1881 stimulation. Less effects were seen with the PR and progestin treatment and only a small increase was observed consecutive to GR and glucocorticoid treatment. The inductions seen were always higher in presence of the shorter construct.

Altogether the data indicate that *Pem* is a direct target gene of the AR and that the corresponding regulatory elements are present in the proximal promoter region. They also show that the *Pem* promoter is preferentially responsive to AR as opposed to GR and PR. This is in contrast to most other androgen-regulated genes including the *PSA* and *C3* gene for which a much stronger response to GR than to AR has been reported (Cleutjens et al., 1997; Rundlett and Miesfeld, 1995).

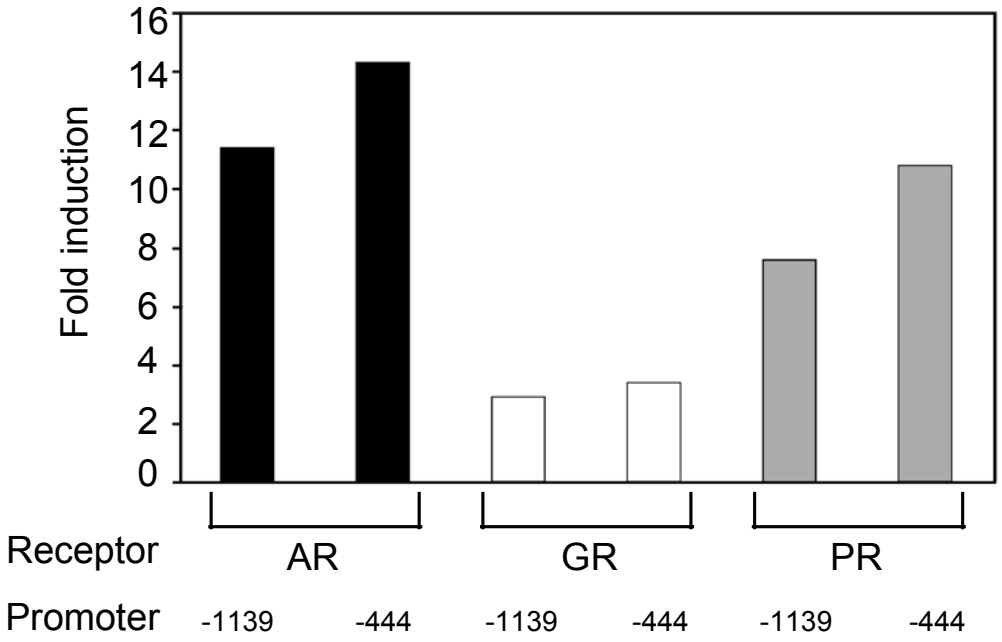

Figure 7: Preferential androgen stimulation of the Pem promoter. *The upstream region of the Pem gene starting at position –1139 or –444 was placed in front of the luciferase reporter gene. These constructs were transfected into CV-1 cells transiently expressing AR, GR, or PR as indicated. The fold induction in the presence of 10^{-9}M steroid (R1881 for AR, R5020 for PR and dexamethasone for GR) is given. The results are a representative of three separate experiments, each measured as sextuplicate.*

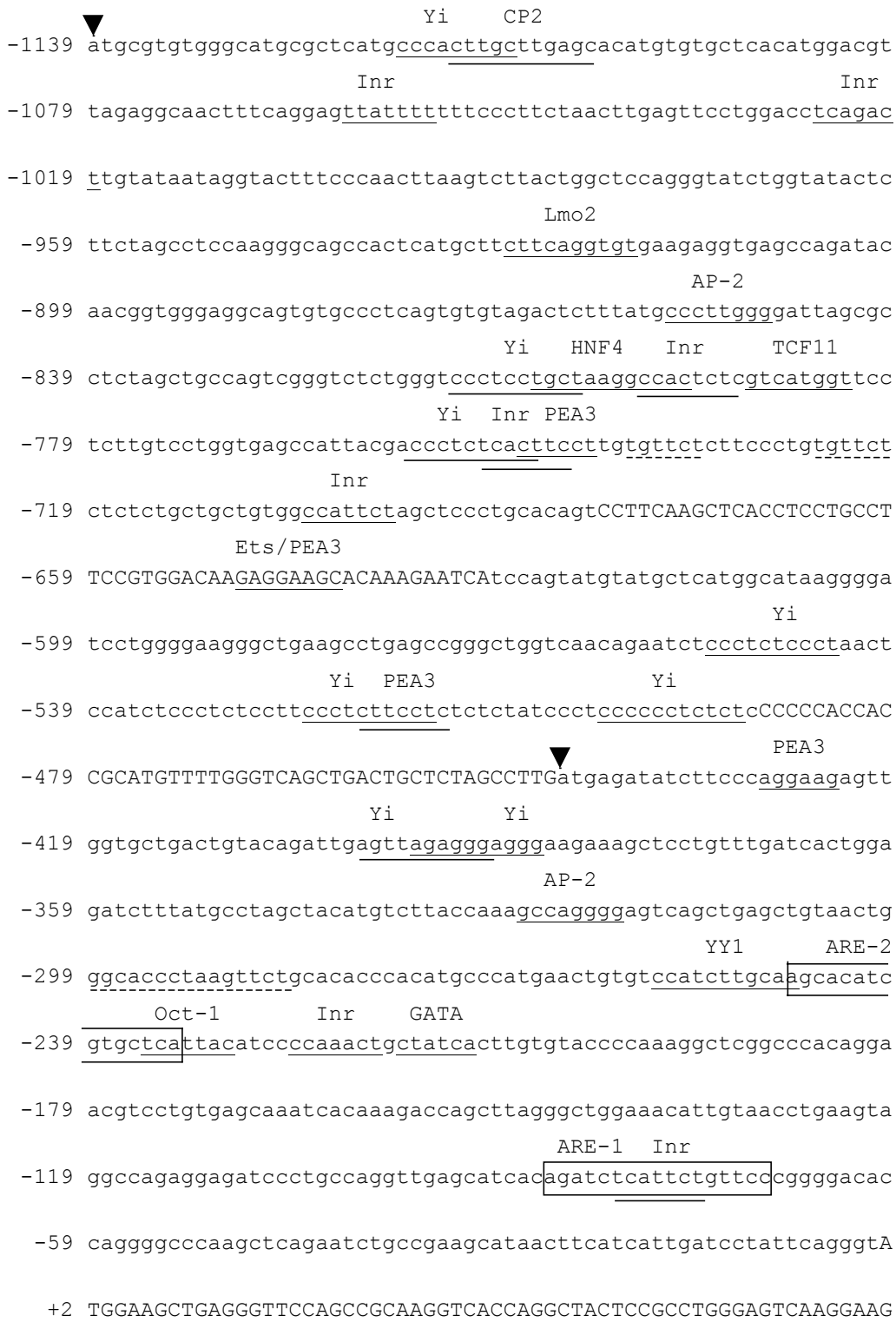

Figure 8: Nucleotide sequence of the mouse Pem promoter. *The putative upstream untranslated exons as well as the first translated epididymal exon are given in capital letters. Numbering starts at the translation initiation codon. Pem ARE-1 and Pem ARE-2 are boxed and the non-binding ARE-like motif as well as half-sites are indicated with a broken line. The potential initiator regions and the motifs matching transcription factor binding sites are underlined. Arrowheads indicate the beginning of the two promoter constructs analyzed in transactivation assays. GenBank accession number: AF410462.*

2.1.1.2. Putative cis-acting elements of the murine Pem promoter

A search for putative regulatory elements was carried out in the murine *Pem* upstream region (Figure 8). No sequence closely matching the consensus SRE AGAACAnnnTGTTCT was found. Two TGTTCT half-sites were located starting at position -739 and -725. They were however upstream of the proximal promoter region previously shown to be responsible for androgen control in the rat *Pem* gene and no sequence resembling a second half-site was found in the vicinity (Sutton et al., 1998). When allowing for more variations in the consensus response element, three candidate motifs could be pinpointed in the proximal promoter: GGCACCctaAGTTCT, AGCACAtcgTGCTCA and AGATCTcattcTGTTCC, starting at positions -299, -247 and -85, respectively. All contained two variant copies of the canonical SRE half-site including the G and C contact nucleotides. These half-sites were spaced by either three or five nucleotides. These putative response elements were further analyzed (see below).

As previously noted in the rat, the mouse *Pem* gene had no TATA box. Several stretches resembling the initiator regions often used in TATA-less genes (Smale, 1997) were found in the upstream region (Figure 8). In addition, motifs with a perfect match to several other DNA regulatory elements were identified in one or the other orientation. Using the PatSearch tool (Heinemeyer et al., 1998), consensus binding sites for Yi, CP2, Lmo2, AP-2, HNF4, TCF11, Ets/PEA3, YY1, Oct-1 and the GATA factor were found (Figure 8).

2.1.1.3. Pem ARE-1 and Pem ARE-2 are bound by the AR in vitro

To test whether the putative response elements were specifically bound by the AR, Barbulescu et al. (2001) performed electrophoretic mobility shift assays (EMSA) with *in vitro* translated full-length human AR. It was thus shown that the -85 and the -247 elements but not the -299 motif displayed specific binding to the AR. The two functional elements were named Pem ARE-1 and Pem ARE-2, respectively. These data were confirmed using AR prepared from nuclear extracts of PC3/ARwt cells, which were incubated with biotinylated oligonucleotides corresponding to the –85 and –247 elements (Figure 11, lanes: Pem ARE-1 and Pem ARE-2). Specific binding of the AR was obtained in both cases. Interestingly, a weaker binding of the AR to the Pem response elements as compared to different SREs was observed (Figure 11, lanes: SRE).

2.1.1.4. The androgen response of the Pem promoter is mediated by both Pem ARE-1 and Pem ARE-2

In order to determine the respective roles of each response element in the androgen regulation of *Pem*, site-directed mutagenesis of the proximal promoter was carried out. The resulting reporter plasmids were analyzed in CV-1 cells transiently expressing the AR or GR (Figure 9). In the presence of AR a strong stimulation by the cognate ligand was seen using the wild-type proximal *Pem* promoter. Less effects were found when using the mutated promoter forms. The Pem ARE-2 promoter mutant displayed 40% and the Pem ARE-1 mutant 65% of the activity of induced wild-type promoter. In a parallel experiment, using CV-1 cells transiently expressing the GR, the wild-type *Pem* promoter was only moderately stimulated by glucocorticoid treatment. Mutation of Pem ARE-1 and even more so of Pem ARE-2 severely lowered the response.

This demonstrates that the two DNA response elements identified in the *Pem* promoter are essential for the androgenic regulation. It furthermore shows that the residual response of the *Pem* promoter to glucocorticoids is mediated by the same response elements.

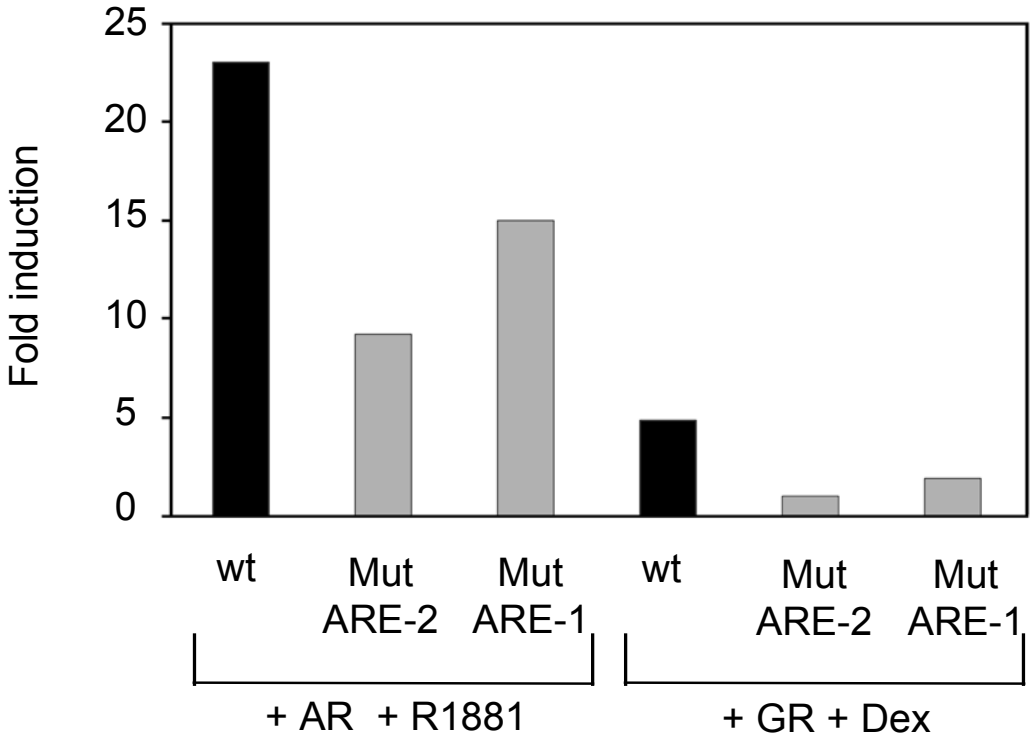

Figure 9: Mutational analysis of the Pem promoter. *Reporter constructs containing the Pem proximal promoter as wild-type (wt) or with mutated Pem ARE-1 (Mut ARE-1) or mutated Pem ARE-2 (Mut ARE-2) were used to transfect CV-1 cells together with an expression vector for AR or GR, as indicated. The fold induction in the presence of 10^{-9}M steroid (R1881 for AR and dexamethasone (Dex) for GR) is given. The results are a representative of three separate experiments, each measured as sextuplicate.*

2.1.2. DNA response elements are modulators of AR action

2.1.2.1. DNA elements specify the preferential transcriptional response to AR, PR or GR

Even though AR, PR and GR all recognize the same consensus SRE, each regulates a distinct set of target genes implying that discrete variations in the DNA sequence might be instrumental for the selectivity of response.

Name	Sequence	Reference
Cons SRE	GGAACAnnnTGTTCT	Nelson et al., 1999
CRISP-1 SRE	GGTACAtctTGTTCA	Schwidetzky et al., 1997
2.43 SRE	GGAACAaaaTGTCCC	Roche et al., 1992
Pem ARE-2	AGCACAtcgTGCTCA	This work
Pem ARE-1	AGATCTcattcTGTTCC	This work

Table 2: DNA sequence of AR-selective and non-selective response elements. *The nucleotide sequences of the five different DNA response elements used in this study are given in 5' to 3' orientation. The half-sites are in uppercase letters, the spacing in lowercase letters.*

To test this hypothesis, androgen response elements were compared (Table 2). Pem ARE-1 and Pem ARE-2 from the *Pem* promoter were analyzed. The response element located at position –1253 of the gene promoter of the secreted epididymal protein CRISP-1 was additionally chosen (Schwidetzky et al., 1997). Finally two sequences identified by *in vitro* selection based on strongest AR binding, namely the 2.43 SRE and the consensus SRE (Roche et al., 1992; Nelson et al., 1999) were also analyzed. Reporter constructs containing two copies of each element were introduced into CV-1 cells together with expression vectors for different steroid receptors. Treatment was with the cognate agonistic ligand (Figure 10). When cotransfecting an AR expression vector and stimulating with R1881, Pem ARE-1 and ARE-2 were found to transmit a much higher response than 2.43 SRE, CRISP-1 SRE or the consensus SRE. In presence of PR and R5020 the stimulation was in the same range for all elements. Finally, in presence of GR and dexamethasone, the 2.43 SRE, CRISP-1 SRE and consensus SRE were the best responders. When comparing the individual responses to the different steroids, Pem ARE-1 and ARE-2 displayed the highest AR selectivity of all elements tested, especially in comparison

to GR effects (10- and 5.5-fold selectivity, respectively). In contrast, the 2.43 SRE, CRISP-1 SRE and consensus SRE were all mainly stimulated by the GR.

The results show that androgen stimulates response elements with only small variations in their DNA sequence to different extents. They also allow the definition of two classes of elements, the AREs which exhibit a selective response to androgen stimulation when compared to glucocorticoid treatment (Pem ARE-1 and ARE-2), and the SREs which are mainly responsive to the GR (2.43 SRE, CRISP-1 SRE and consensus SRE).

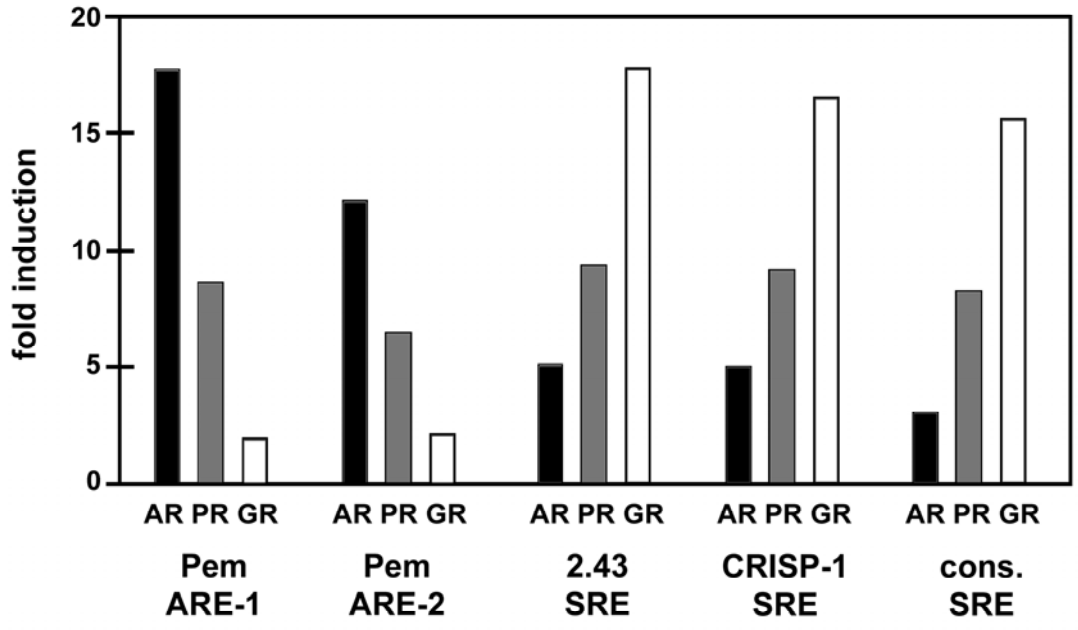

Figure 10: Selectivity of DNA response elements for steroid receptors. *Reporter plasmids carrying two copies of the indicated DNA elements were cotransfected with expression vectors for AR, PR or GR into CV-1 cells. The fold induction following treatment with R1881 (black bars), R5020 (grey bars) or dexamethasone (white bars) is given. The results are a representative of three separate experiments each measured as sextuplicate values.*

2.1.2.2. Binding affinity of response elements to AR does not correlate with transactivation potential

In order to determine whether the preferential androgen response of the selective elements correlated with stronger AR binding, complexes formed of DNA elements bound by AR and associated proteins were isolated from PC-3 cells stably expressing the full-length human AR (in cooperation with Dr. H.A. Meyer, Schering AG). Biotinylated oligonucleotides containing the various response elements as tandem repeat and coupled to streptavidin beads were used as baits for the purification. They were first incubated with nuclear extracts prepared from PC-3/AR cells treated with R1881. Non-specifically bound proteins were then removed by washing before eluting bound AR complexes with high-salt buffer. The amount of released AR was assessed by Western blot analysis, using an antibody directed against the N-terminal domain (Figure 11). The results showed that significantly more AR was associated to the three non-selective than to the two AR-selective elements, indicating that preferential androgen stimulation was not due to stronger AR binding.
Since the consensus SRE and CRISP-1 SRE differed in only one base pair of their half-site and behaved identically in transactivation assays and binding studies, only one of them was used in the subsequent experiments.

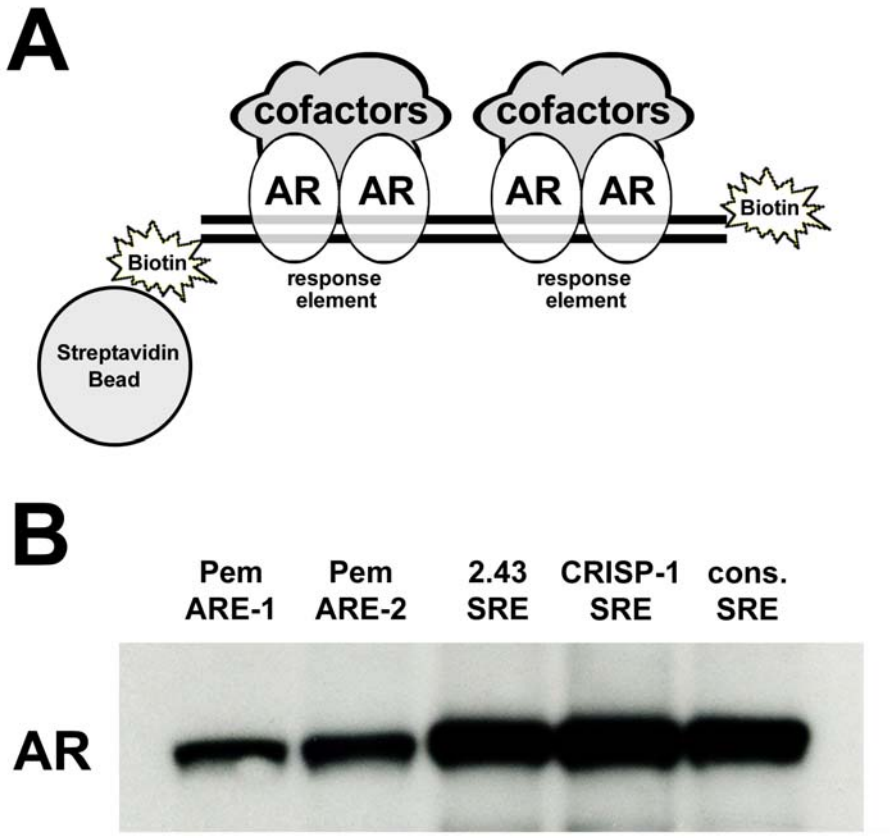

Figure 11: Isolation of DNA response element/protein complexes. *(A) Schematical representation of the strategy used to purify response element/AR protein complexes. (B) Characterization of purified complexes. The amount of AR bound to different response elements was determined by Western blot using a specific antibody directed against the N-terminal domain of AR.*

2.1.2.3. Distinct AR protease digestion patterns result from binding to different response elements

In order to find out whether DNA response elements influenced the conformation of bound AR, we performed protease digests. Protein/DNA complexes were purified through the biotin tag attached to the response elements to ensure that only DNA-bound AR was obtained. These complexes were then submitted to partial digestion using chymotrypsin or trypsin. The reaction products were separated on a denaturing gel and the bands corresponding to digested AR were detected by an antibody recognizing the C-terminal moiety. As observed above, more AR was associated to the SREs than to the AREs in the undigested complexes (Figure 11 and 12 A and B, 0 ng/µl protease, lanes 1 and 2 compared to lanes 3 and 4). Some digestion products closely reproduced this pattern so that a differential sensitivity to proteases could not necessarily be inferred. There were however instances where more product was formed from the ARE complex than from the SRE complex. Using chymotrypsin at a concentration of 0.2 ng/µl, a rapid degradation of AR associated to the selective elements was apparent for band C1 (Figure 12 A, lanes 3 and 4) whereas only a very weak band corresponding to intact AR remained (band AR). Considering that more AR associated to the non-selective elements was originally present, the product C1 was proportionally less represented than in the samples where ARE-bound complexes were analyzed (lanes 3 and 4). Also, the fact that a band of lower molecular weight (C2) exhibited a pattern opposite to that of C1 indicated that the ARE-bound complexes were not altogether more accessible to chymotrypsin. Using trypsin at a concentration of 2 ng/µl, a prominent digestion product labeled T1 was generated from selective element-bound complexes (Figure 12 B, lanes 3 and 4) but was less apparent for the non-selective elements (lanes 1 and 2). The opposite pattern was seen for a digestion product with a lower molecular weight (band T2). This band was stronger for the non-selective than for the selective elements (lanes 1 and 2 compared to lanes 3 and 4).

The inverted ratios seen for the bands AR and C1 or T1 and T2 originating from complexes bound to selective or non-selective elements indicate that differences in protease sensitivity exist for the AR, depending on the bound DNA. This suggests element-induced alterations in AR conformation, in the set of associated cofactors, or in both.

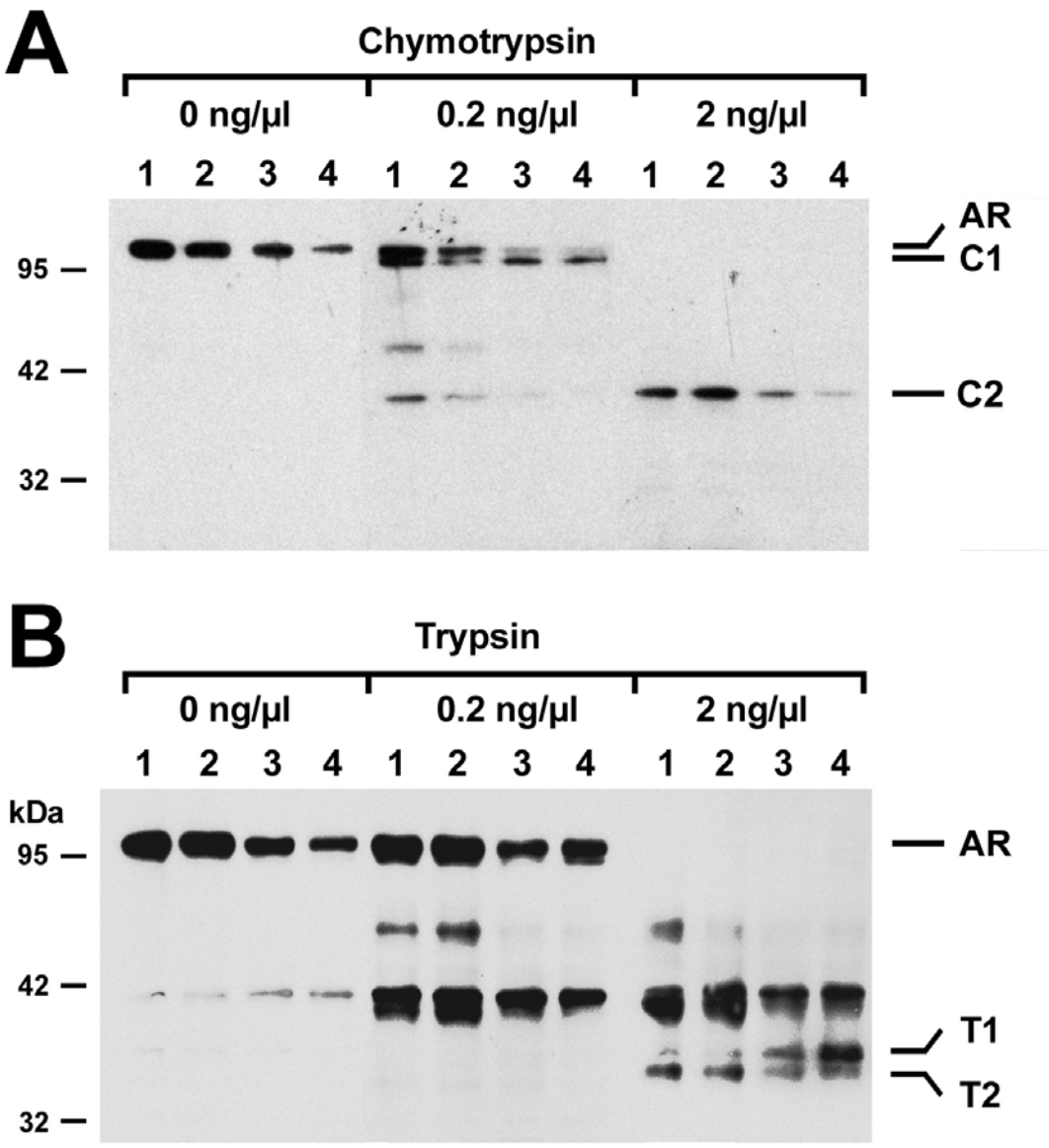

Figure 12: Protease digestion patterns of AR attached to DNA elements. *Response element/protein complexes were purified from nuclear extracts prepared from PC-3/AR cells and digested using the indicated amounts of chymotrypsin or trypsin. Total protein concentration was identical for all elements. Lane 1, consensus SRE; lane 2, 2.43 SRE; lane 3, Pem ARE-2; lane 4, Pem ARE-1. The AR digestion patterns were visualized using a specific antibody directed against the C-terminal end of the LBD of the AR. The digestion products discussed in the text are indicated (C1, C2, T1, T2). The results are a representative of three separate experiments.*

2.1.2.4. Mutations in the dimerization box differentially affect AR transactivation potential via different response elements

An opposite half-site orientation (direct versus inverted repeat) of AR-selective as opposed to non-selective DNA elements as well as an assymetrical mode of recognition by the AR have been reported (Claessens et al., 2001; Barbulescu et al., 2001). These observations and the different protease digestion patterns obtained in this study suggest that the AR homodimer adopts a different conformation, depending on the bound element class. This in turn may impinge on the role of domains directly implicated in receptor dimerization. The second zinc finger of the DBD and especially its D box have been shown to partake in the dimerization interface of steroid receptors (Figure 13; Luisi et al., 1991). From the crystal structure of the GR DBD and from mutagenesis experiments, it is known that two charged amino acids of the D box are engaged in intermolecular salt bridges (Luisi et al., 1991). Mutation for a residue of the opposite charge disrupts this interface, leading to a dramatic loss of activity on a single DNA element but, surprisingly, to an enhanced activity on multiple elements (Liu et al., 1996).

The equivalent mutation where an arginine was exchanged for an asparagine, R598D and the opposite mutation D600R were introduced into the AR (Figure 14 A). The activity of each mutant was compared to that of wild-type AR following transfection into CV-1 cells and using reporter plasmids harboring the different response elements as tandem repeats (Figure 14 B). AR D600R activity in transactivation assays was similar to that of wild-type AR in presence of Pem ARE-1 and Pem ARE-2, but was twice enhanced in presence of CRISP-1 SRE and 2.43 SRE. With AR R598D, the effects were much more pronounced. Here, a doubling of activity was seen in presence of the Pem elements and a 8- to 9-fold increase for the other elements, when compared to wild-type AR. Western blot analysis showed that the expression levels of wild-type AR and AR mutants were comparable following transfection into CV-1 cells (Figure 14 B, inset).

Another residue of the D box implicated in AR dimerization is A596 (Figure 14 A). Its mutation from alanine to threonine has been discovered in patients suffering from Reifenstein syndrome, a disease characterized by partial androgen insensitivity (Kaspar et al., 1993). The activity of AR A596T mediated by the different elements present as tandem repeats was determined (Figure 14 C). For the Pem elements, a decreased activity of AR A596T in comparison to wild-type AR was measured. In

contrast, little change was seen when testing the CRISP-1 SRE and more than a fivefold increase for the 2.43 SRE. Western blot analysis indicated the level of AR A596T to be lower than that of wild-type AR (Figure 14 C, inset), so that the enhancement observed might be an underestimation.

Altogether these results show that disruption of the DBD dimerization box is still compatible with AR function and that in some cases it even leads to enhanced activity. They additionally show the role of this interface to greatly vary, depending on the recognized DNA element, in line with a different arrangement of the bound AR homodimer.

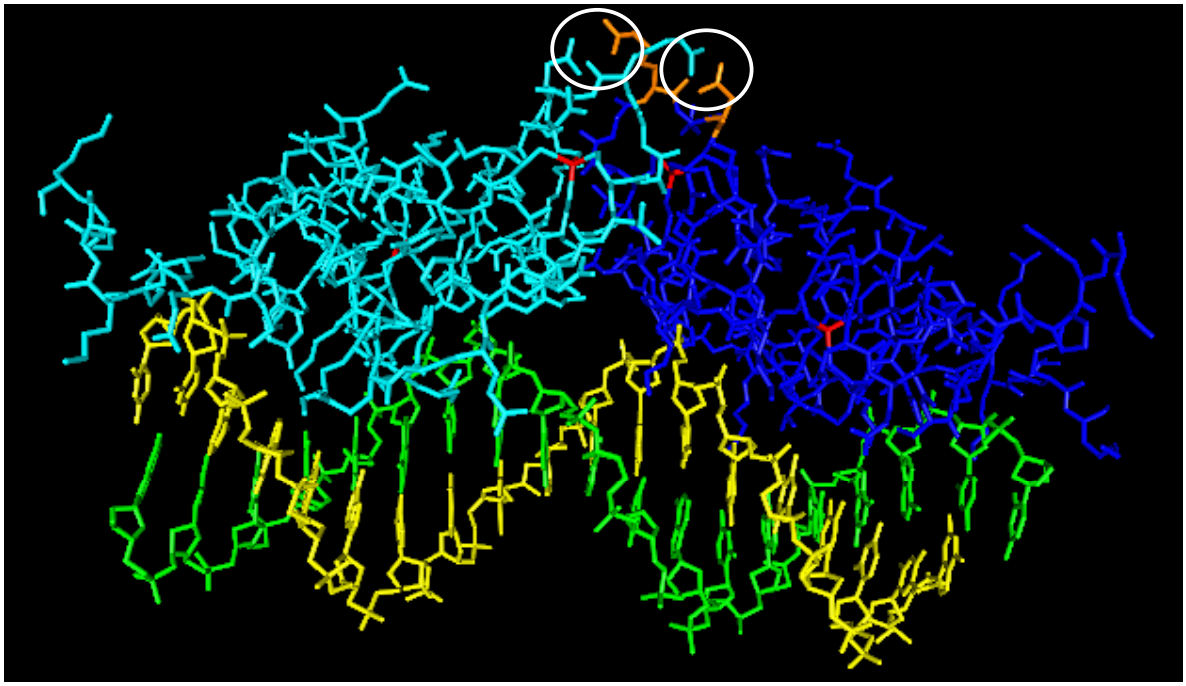

Figure 13: Three dimensional structure of the GR DBD homodimer bound to DNA. *The homodimer of two GR DBDs (light and dark blue) bound to double-stranded DNA (green and yellow) is shown (derived from Luisi et al., 1991). The salt bridges formed between the monomers by R460 and D462 are marked by white circles. The R460 and D462 residues of the dark blue GR monomer are colored orange. The zinc atoms are in red.*

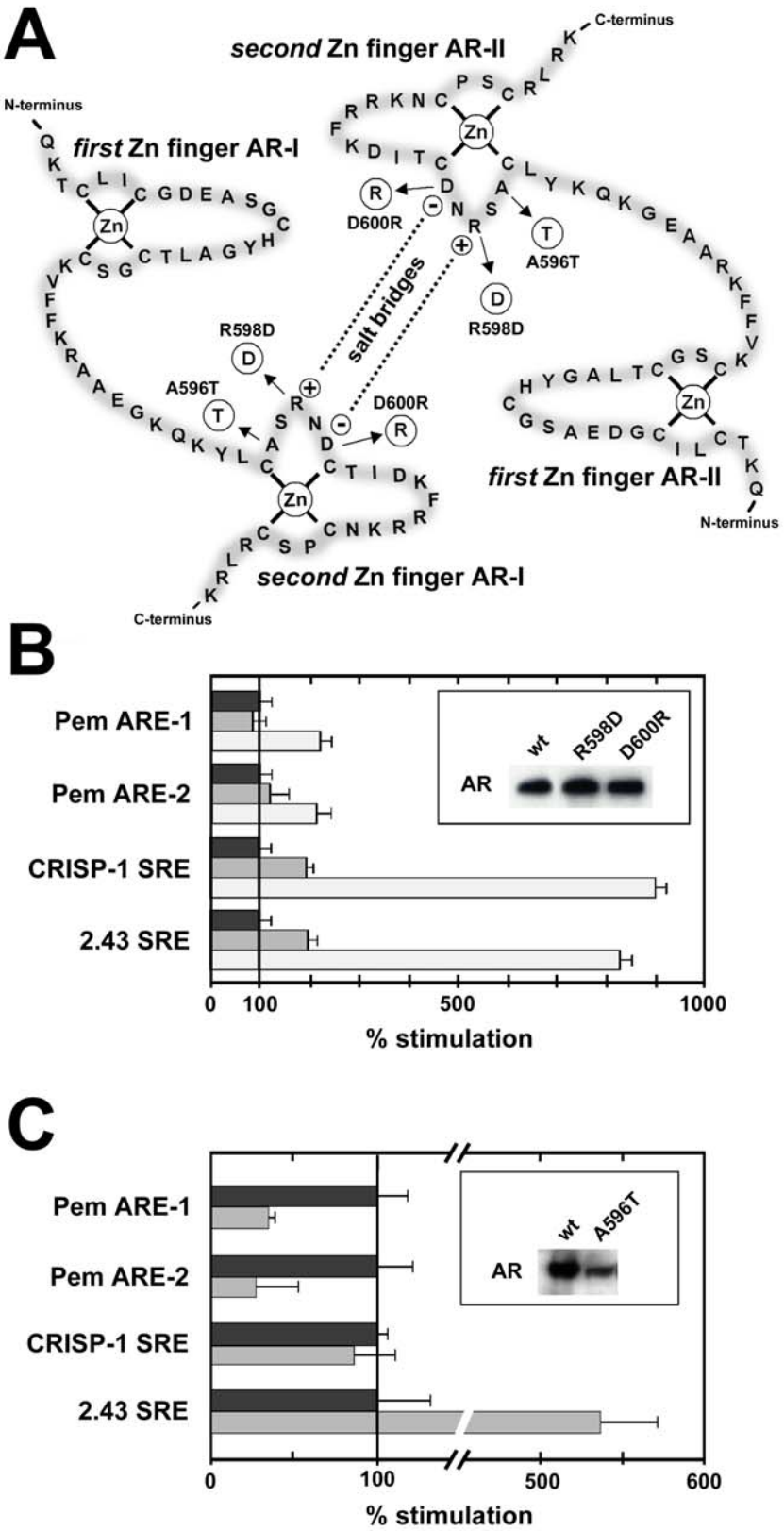

Figure 14: Role of the DBD dimer interface in AR transactivation depends on the response elements. *(A) Schematic drawing of AR homodimer salt bridges. The AR DBD of each monomer is given. Potential salt bridges are indicated with dotted lines. Positions of the*

A596T, R598D and D600R mutations are shown. (B), Reporter plasmids carrying two copies of the indicated elements were cotransfected into CV-1 cells together with an expression plasmid for wild-type AR (black bars), AR D600R (grey bars) or AR R598D (light grey bars). (C), Reporter plasmids carrying two copies of the indicated elements were cotransfected into CV-1 cells together with an expression plasmid for wild-type AR (black bars) or AR A596T (grey bars). The fold induction obtained with R1881 was set to 100%. The results are a representative of three separate experiments and the bars are the mean ±SEM of sextuplicate values. Inset: Western blot analysis of transfected CV-1 cells using an AR-specific antibody.

2.1.2.5. The coactivators TIF2 and ARA55 differentially modulate AR activity depending on the response elements

Next it was examined whether the different conformations elicited by binding to DNA elements affected AR response to cofactors. TIF2 and ARA55 stimulate the ligand-dependent activity of the AR and of other steroid receptors (Heinlein et al., 2002). CV-1 cells were cotransfected with reporter plasmids containing two copies of the different DNA elements and expression plasmids for the AR and the coactivators TIF2 or ARA55. In the control experiments, the same amount of expression vector containing a neutral insert was added. For both cofactors and for all elements tested, enhancement of androgen-driven transcriptional activity was noted (Figure 15). A peak at 0.1 nM followed by a small decline of stimulation was observed for TIF2 (Figure 15, left column). This was not the case for ARA55 where increase of stimulation was seen at least up to 1-10 nM ligand concentrations, above which a plateau effect was noted (Figure 15, right column). Altogether more stimulating effects were observed on ARE- than on SRE-mediated AR action, in line with the stronger activity of AREs in absence of added cofactor.

Thus, both TIF2 and ARA55 enhance ligand-dependent AR activity via all DNA elements, with more pronounced effects on AREs. This strongly suggests that cofactor action is affected by the modulatory effects of DNA elements on AR conformation.

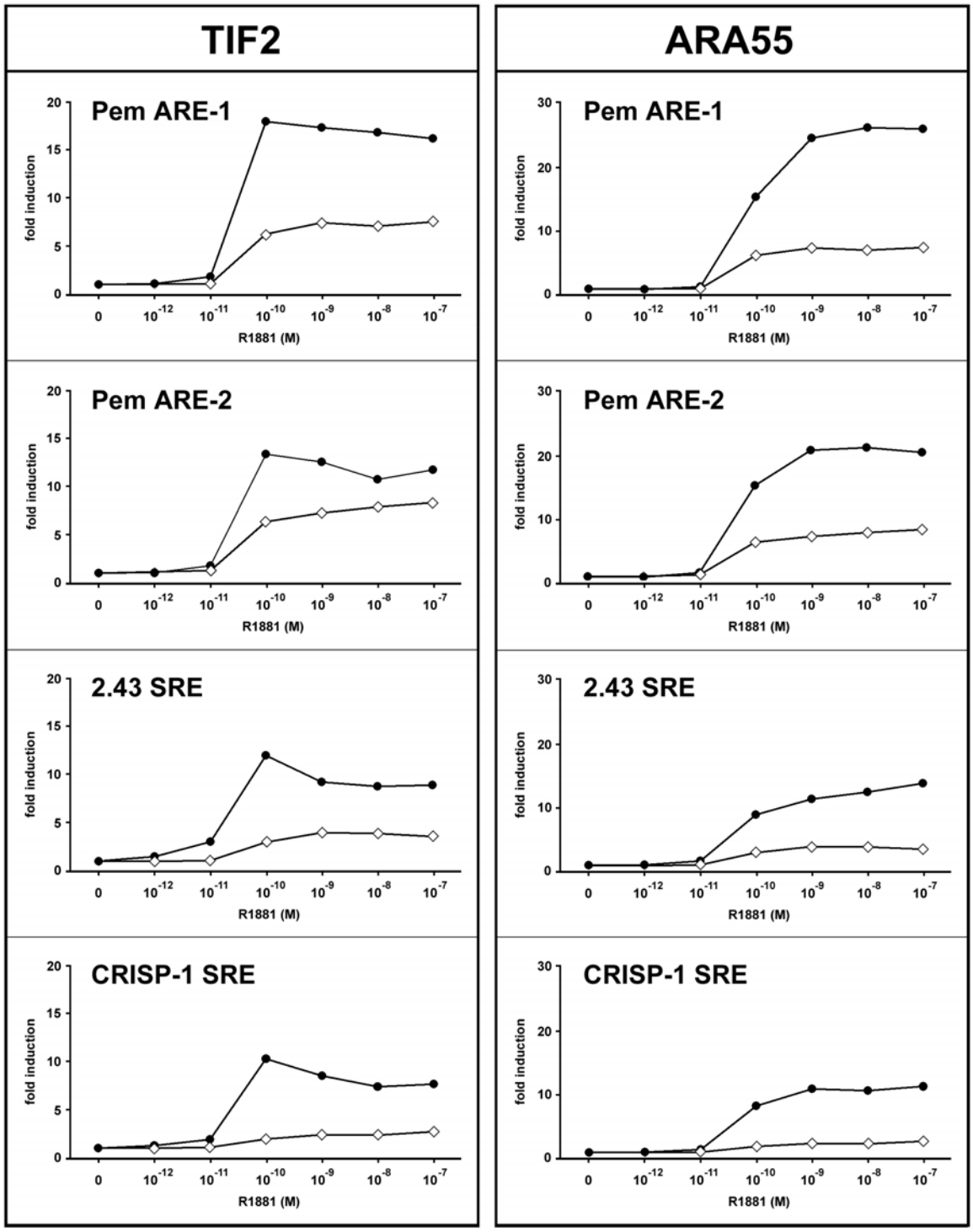

Figure 15: Effects of TIF2 and ARA55 overexpression on AR function mediated by different DNA elements*. CV-1 cells were cotransfected with a reporter gene carrying two copies of Pem ARE-1, Pem ARE-2, CRISP-1 or 2.43 SRE and expression vectors for AR and TIF2 (left column) or ARA55 (right column). The concentrations of R1881 used for treatment are indicated. The fold induction measured in presence of the TIF2- or ARA55-encoding plasmid (black dots), or of the β-galactosidase-encoding plasmid (white diamonds) are given. Each point is the mean of two independent experiments for which sextuplicate values were determined.*

2.1.2.6. Sumoylation enzymes modulate AR function in a DNA element-dependent fashion

Post-translational modifications have been reported to affect AR function. Sumoylation is the covalent conjugation of the SUMO amino acid chain to Lys at specific sites of target proteins. Two such sites are known in the AR, K386 and K520, three in the GR, one in the PR and none in the ER. For the AR, sumoylation may either stimulate or repress AR activity, depending on the experimental setting (Kotaja et al., 2002; Nishida et al., 2002). Recent data indicate that Ubc9 and the PIAS family are involved in the process of sumoylation as SUMO conjugase and ligases, respectively (Kotaja et al., 2002; Nishida et al., 2002; Poukka et al., 1999; Poukka et al., 2000). Using cotransfection experiments as above, the effect of ectopic Ubc9 or PIASxα expression on AR function mediated by various response elements was analyzed. When overexpressing Ubc9, a differential effect was observed on AREs as compared to SREs (Figure 16, left column). AR action transmitted by SREs was stimulated at all hormone concentrations above 0.01 nM, with a peak at 0.1 nM. Conversely, little effect was noted on Pem ARE-1 and a repression on Pem ARE-2. When overexpressing PIASxα, virtually no change in AR stimulation was visible at any ligand concentration for the non-selective elements. Conversely, a marked inhibitory effect on AR activity mediated by the selective elements was observed at 0.1 nM and higher androgen concentrations (Figure 16, right column).

Altogether these data show the effects of Ubc9 on AR function to greatly vary, depending on the response elements tested. Ubc9 enhances AR activity transmitted by non-selective elements but not by selective elements. Conversely, PIASxα does not significantly affect AR activity conveyed by non-selective elements but significantly represses it in presence of selective ones. It can therefore be concluded that the modulatory effects of two enzymes involved in the sumoylation pathway are differently interpreted by DNA response elements.

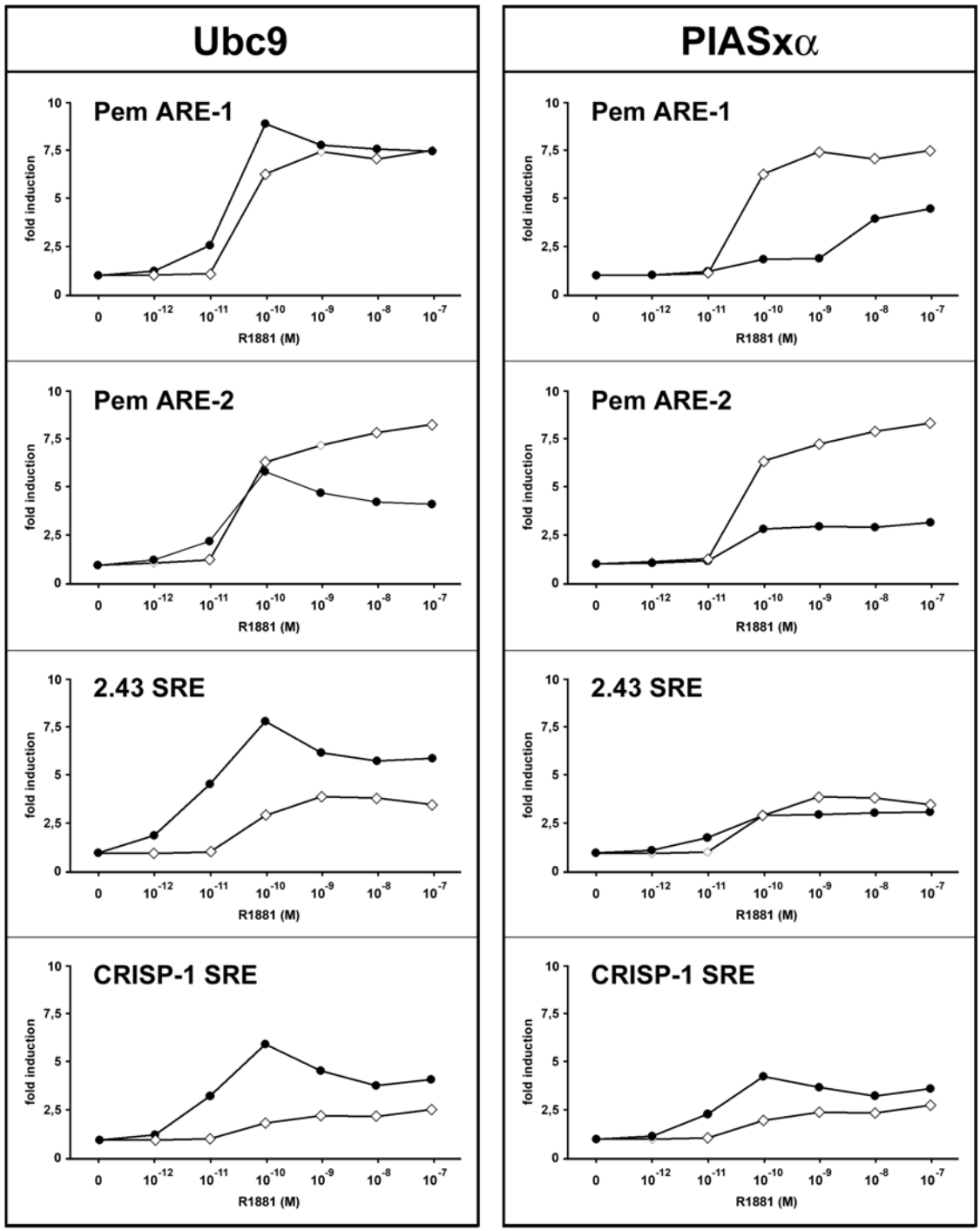

Figure 16: Effects of Ubc9 and PIASxα overexpression on AR function mediated by different DNA elements. *CV-1 cells were cotransfected with a reporter gene carrying two copies of Pem ARE-1, Pem ARE-2, CRISP-1 or 2.43 SRE and expression vectors for AR and Ubc9 (left column) or PIASxα (right column). The concentrations of R1881 used for treatment are indicated. The fold induction measured in presence of the Ubc9- or PIASxα-encoding plasmid (black dots), or of the β-galactosidase-encoding plasmid (white diamonds) are given. Each point is the mean of two independent experiments for which sextuplicate values were determined*

2.1.3. Mechanisms specifying AR, PR, and GR selectivity

A critical problem within the steroid receptor family is how AR, PR and GR specifically activate their target genes, even though they all recognize the same consensus DNA element. Having established that two classes of response elements exist for the AR and that subtle changes in their sequence affect the conformation of bound AR, it was interesting to study how the mode of action of PR and GR in mediating transcriptional control differed from that of the AR.

2.1.3.1. Element-specific synergy effects contribute to receptor selectivity

More than one DNA response element is typically found in naturally occurring steroid-dependent promoters. The effect of steroid receptors on these elements can be additive or synergistic. For example the GR is known to self-synergize on multimerized SREs (Liu et al., 1996). To test whether AR and PR were also capable to synergize and to establish if such an effect was dependent on the DNA element, the transactivation mediated by reporter constructs containing one or two copies of a given response element were compared (Figure 17). CV-1 cells were transfected with an AR, PR, or GR expression plasmid and a reporter plasmid, and treated or not with the appropriate hormone. The fold inductions measured for the hormone-induced samples in presence of single or tandem repeat elements were compared to determine the synergy index. A ratio of 2 indicates that only additive effects had taken place whereas above 2 synergistic effects can be inferred. AR and PR showed strong synergy on the Pem AREs, whilst only additive effects were found on the non-selective SREs (Figure 17). With a ratio above ten, Pem ARE1 in combination with AR exhibited the highest synergy measured. In contrast to AR and PR, GR did not display effects, with the exception of CRISP-1 SRE for which an index of 3 was calculated.

Altogether these results show that self-synergy effects vary between the AR, PR and GR, and are highly dependent on the DNA response element.

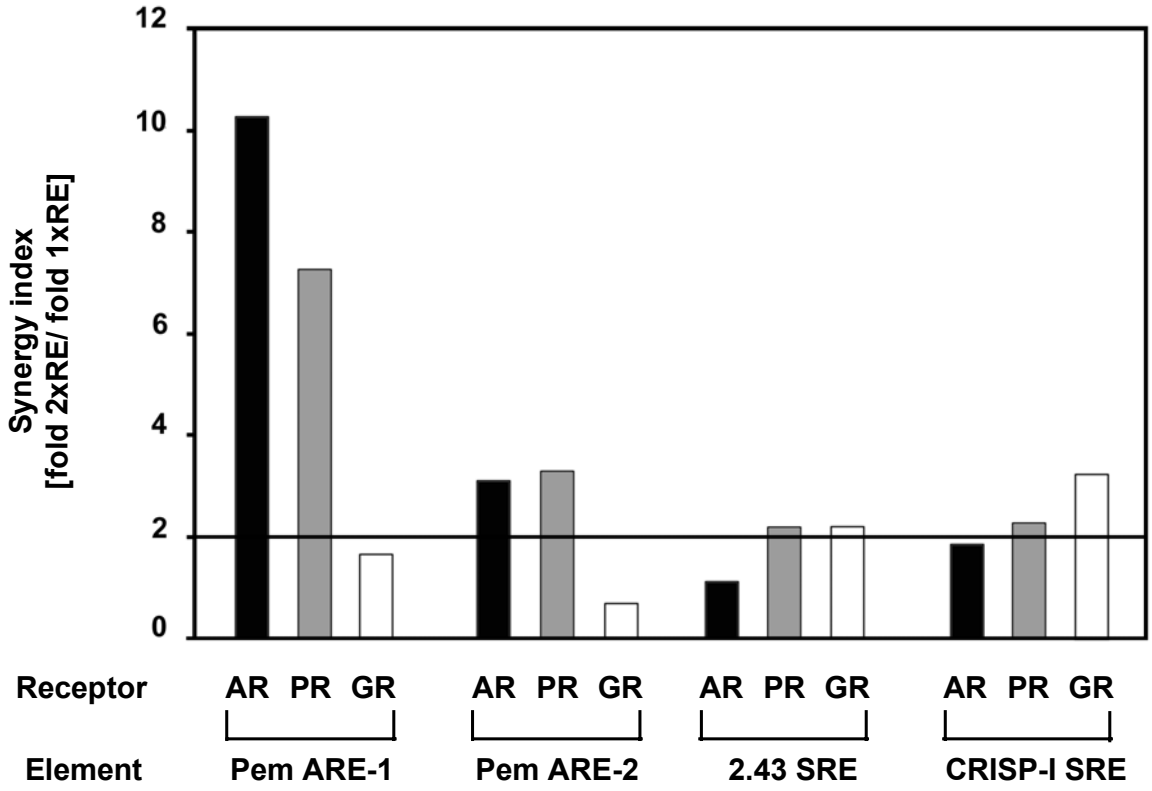

Figure 17: Response elements determine receptor synergy. *Reporter plasmids carrying one or two copies of the indicated elements were cotransfected into CV-1 cells together with an expression plasmid for AR (black bars), PR (grey bars) or GR (white bars). The fold induction obtained with the appropiate ligand for the plasmids containing two elements was divided by the fold induction obtained with the plasmid containing one element, thus giving the synergy index. The black line indicates the threshhold value of two, above which synergy is present. The results are a representative of three separate experiments each measured in sextuplicate values.*

2.1.3.2. Mutations in the PR and GR DBD have a different impact on transactivation potential than the equivalent AR mutations

Mutations in the highly conserved D box of the DBD have recently been reported to enhance the synergy and transactivation potentials of GR (Liu et al., 1996; Iniguez-Lluhi et al., 2000) and of AR (Chen et al., 1997). Because synergy was found to depend not only on the receptor but also on the response element (see above), the effects of equivalent D box mutations for AR and PR activities were compared (see also section 2.1.2.4. and Figure 14).

CV-1 cells were transfected with the receptor expression constructs and the different reporter plasmids, and treated or not with hormone (Figure 18). Similarly to the AR and GR mutants (Liu et al., 1996; Iniguez-Lluhi et al., 2000; Chen et al., 1997), the PR R606D and PR D608R mutants had a higher transactivation potential on the classical CRISP-1 SRE than wild-type PR had (Figure 18). Like for GR and AR, the effect was more pronounced for the PR R606D mutation than for the PR D608R mutation. For the SRE 2-43 element, the D box mutations did not affect the transactivation potential of the PR in any direction, in contrast to what was seen with the AR. The androgen-selective AREs which are weakly activated by wild-type GR and intermediately by wild-type PR (see Figure 10) were stimulated by the PR mutants to only about 50% of control levels. This is in contrast to the effects seen with the AR D box mutants.

Another conserved amino acid in the D box is the Ala residue following the first Cys of the second zinc finger. As already described above, the AR A596T mutation does not modify its activity on non-selective SREs, whereas it markedly reduces it on the selective AREs. The homologous changes were introduced into the PR (PR A604T) and GR (GR A458T), and the resulting mutants were tested in parallel to AR A596T on four different response elements (Figure 19). The GR A458T mutant displayed a decreased activity as compared to wild-type GR on both the SREs and the AREs. Similarly to the GR, the PR A604T displayed decreased activity on all tested elements. This mutation of the D box thereby led to a decreased transactivation potential of all three receptors on the AREs. On the SREs however, only the PR and GR mutants but not the AR mutants displayed reduced activity.

The different effects of the equivalent mutations introduced into the DBD of the three steroid receptors indicate that the function of the highly conserved D box is distinct in the AR, PR and GR. It might thus be important for the selective responses displayed by different DNA elements to receptor stimulation.

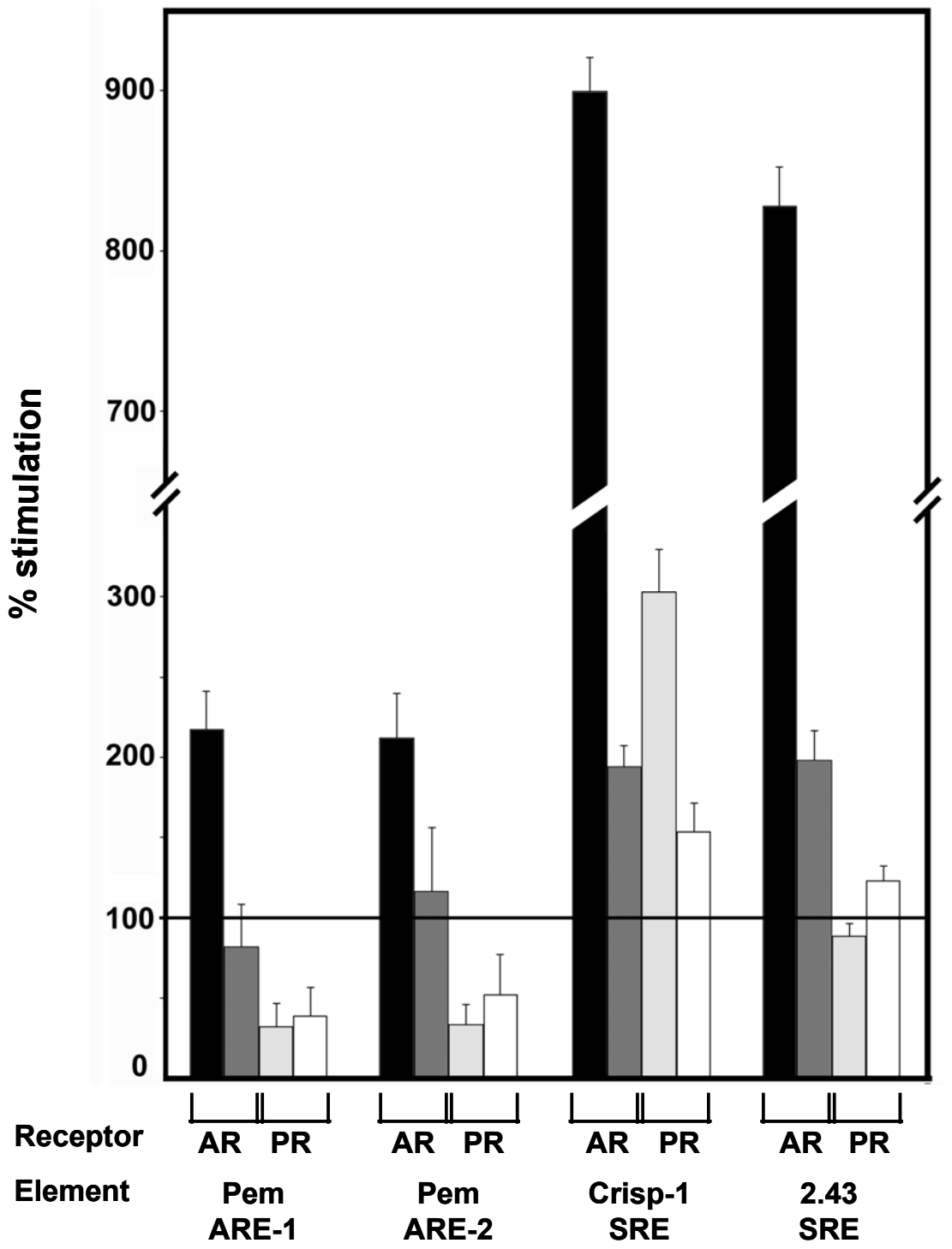

Figure 18: AR and PR transactivation potentials differently depend on their DBD-dimerization interface. *Reporter plasmids carrying two copies of the indicated elements were cotransfected into CV-1 cells together with an expression plasmid for wild-type AR, AR R598D (black bars), AR D600R (dark grey), wild-type PR, PR R606D (light grey bars) or PR D608R (white bars). The fold induction obtained with R1881 for wild-type AR or with R5020 for wild-type PR was set to 100%. The results are a representative of three separate experiments measured as sextuplicate values.*

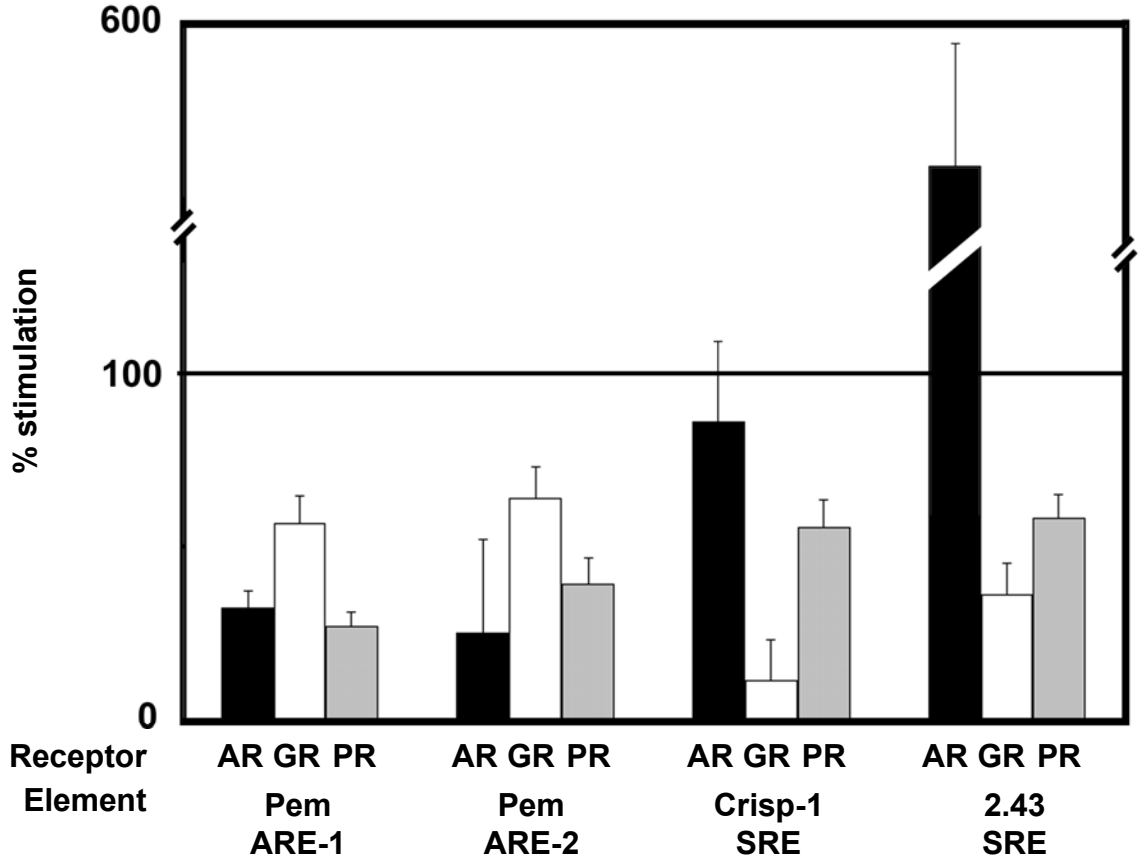

Figure 19: Role of the DBD dimer interface in AR, PR and GR transactivation depends on the response elements. *Reporter plasmids carrying two copies of the indicated elements were cotransfected into CV-1 cells together with an expression plasmid for wild-type AR, AR A596T (black bars), wild-type GR, GR A458T (white bars), wild-type PR and PR A604T (grey bars). The fold induction obtained with R1881 for wild-type AR, dexamethasone for wild-type GR or R5020 for wild-type PR was set to 100%. The results are a representative of three separate experiments measured as sextuplicate values.*

2.2. *OTEX*, an androgen-regulated human member of the *paired*-like class of homeobox genes

Only a few target genes that mediate the effects of the AR during male sexual development, in fertility or prostate cancer are known to date. Recently, an androgen-regulated homeobox gene named *Pem* and expressed in embryonic tissues and in adult epididymis and testis has been described in rat and mouse (Maiti et al., 1996b; Lindsey et al., 1996). *Pem* belongs to the *PEPP* sub-family of *paired*-like homeobox genes and possibly functions as a transcription factor transmitting the signals of the AR and regulating the expression of a unique set of genes. The identification of human members of the *PEPP* family including the orthologue of rodent *Pem* could help to better understand the action of the AR in human reproduction and prostate cancer.

2.2.1. Identification and cloning of OTEX cDNA

The screening of public databases allowed the identification of an expressed sequence tag (EST) and of genomic sequences potentially coding for a novel paired-like homeobox protein which was named OTEX (ovary-testis-epididymis-homeobox). Specific primers were devised to amplify the corresponding cDNA from human ovary which was subsequently cloned and sequenced on both strands. In addition, the 5´ and 3´ extremities were reamplified separately from testis and ovary cDNA to check for tissue-specific differences and splice variants, but colinear sequences only differing in length were obtained. The sequence of the longest cDNA clone identified is depicted (Figure 20). An open reading frame coding for a 184 amino acid-long protein was found. The translation start codon was embedded in a sequence fitting with the consensus. An in-frame stop codon was present upstream, indicating that the coding region was complete. A polyadenylation signal was observed near the end of the 3´ untranslated region.

```
    Ov        Ov                    Te
  1 AACTAGCTCCACCCTCTAACCCCCACTCCAGCTGCAGACGCCACGGAGTTTGTGCAGGGG
          Te
 61 CGCAGCGCTCCAGCCATGGCGCGTTCGCTCGTCCACGACACCGTGTTCTACTGCCTGAGT
  1               M  A  R  S  L  V  H  D  T  V  F  Y  C  L  S

121 GTATACCAGGTAAAAATAAGCCCCACACCTCAGCTGGGGGCAGCATCAAGCGCAGAAGGC
 16 V  Y  Q  V  K  I  S  P  T  P  Q  L  G  A  A  S  S  A  E  G

181 CATGTTGGCCAAGGAGCTCCAGGCCTCATGGGTAATATGAACCCTGAGGGCGGTGTGAAC
 36 H  V  G  Q  G  A  P  G  L  M  G  N  M  N  P  E  G  G  V  N

241 CACGAGAACGGCATGAACCGCGATGGCGGCATGATCCCCGAGGGCGGCGGTGGAAACCAG
 56 H  E  N  G  M  N  R  D  G  G  M  I  P  E  G  G  G  G  N  Q

301 GAGCCTCGGCAGCAGCCGCAGCCCCCGCCGGAGGAGCCGGCCCAGGCGGCCATGGAGGGT
 76 E  P  R  Q  Q  P  Q  P  P  P  E  E  P  A  Q  A  A  M  E  G

361 CCGCAGCCCGAGAACATGCAGCCACGAACTCGGCGCACGAAGTTCACGCTGTTGCAGGTG
 96 P  Q  P  E  N  M  Q  P  R  T  R  R  T  K  F  T  L  L  Q  V
                                                        ><
421 GAGGAGCTGGAAAGTGTTTTCCGACACACTCAATACCCTGATGTGCCCACAAGAAGGGAA
116 E  E  L  E  S  V  F  R  H  T  Q  Y  P  D  V  P  T  R  R  E
                                          ><
481 CTTGCCGAAAACTTAGGTGTGACTGAAGACAAAGTGCGGGTTTGGTTTAAGAATAAAAGG
136 L  A  E  N  L  G  V  T  E  D  K  V  R  V  W  F  K  N  K  R

541 GCCAGATGTAGGCGACATCAGAGAGAATTAATGCTCGCCAATGAACTACGTGCTGACCCA
156 A  R  C  R  R  H  Q  R  E  L  M  L  A  N  E  L  R  A  D  P

601 GACGACTGTGTCTACATCGTCGTGGACTAGCCCTAGAATGCCATCCTTCTTCAGGAGCTA
176 D  D  C  V  Y  I  V  V  D  *

661 GTTTGGAGATGGGTTTTTCTGGTGCCACTGACACCTGGGCTGCCCATGCCGCTCAGGCTA

721 CCCTTATCTCCTCTGCACTTATGTTATCAATAAAG
```

Figure 20: Sequence analysis of OTEX. *Nucleotide and predicted amino acid sequences of OTEX cDNA are shown. The 5´ ends of the longest cDNAs obtained from ovary (Ov) or testis (Te) RNA are indicated. The polyadenylation signal is in italics. The exon/intron boundaries are marked with converging arrowheads. The homeobox domain is underlined. The NLS is highlighted in bold letters. The accession number of the sequence in the GenBank/EMBL database is AY099086.*

2.2.2. Sequence analysis of OTEX

Analysis of the deduced OTEX protein sequence revealed the presence of a characteristic 60 amino acid HD (Figure 20; underlined) related to the paired HD (Figure 21). High sequence identities were found with PaxD from the coral *Acropora millepora*, PAX3 and PAX7 from human, and gooseberry from *Drosophila* (Miller et al., 2000). However, unlike these homeobox proteins, OTEX had no Ser at position 50 and did not possess an additional paired domain. This put OTEX in the paired-like family of which the *Drosophila* protein aristaless is the prototype (Galliot et al., 1999). A phylogenetic analysis (Figure 22) indicated that OTEX was a new member of the recently defined PEPP subfamily of paired-like homeobox proteins which comprises Pem, Esx1, Spx1, ESXR1 as well as Psx1 and Psx2 (Maiti et al., 1996a and b). When aligning the HDs, 53.3% sequence identity was calculated with ESXR1, 43.3-45% with Psx1 and Psx2 and 30-31.7% with mouse and rat Pem. A database search and additional phylogenetic analysis identified DNA sequences coding for another human and two more mouse members of the PEPP subfamily: *THG1* (accession number AF317219), *Ehox* (accession number NM_021300) and a RIKEN clone (accession number NM_029203) (Figures 21 and 22). The deduced HDs exhibited 45%, 36.7% and 31.7% sequence identity to the OTEX HD. A phylogenetic tree was constructed in order to compare the relationship between the HDs of the different PEPP family members. THG1, Ehox and RIKEN (NM_029203) were found to belong to a discrete subgroup with highest sequence identity to Psx and Pem. OTEX and more so the Esx subgroup were more distantly related.

A hallmark shared by the HDs of all but one PEPP subfamily members and not observed in other HDs was the presence of an Arg at position 58 (Figure 21). Another frequent feature was the presence at positions 39 and 40 of a Glu and a Val residue. Despite the low overall conservation, the OTEX HD shared additional rare characteristics with the Pem HD, namely the presence of a helix-breaking Pro at position 29 and of a Lys at position 50, a site essential for the DNA-binding specificity of homeobox proteins. P29 has already been described in the more distantly related bicoid and Hox HDs (Treisman et al., 1992; Gehring et al., 1994) whereas K50 was found in Psx2 and Ehox, as well as in the otd/Otx/Crx, Ptx and Gsc families (Galliot et al., 1999). Other residues known to be critical for HD function were maintained in OTEX. Positions 47 and 48 of helix 3 which are essential for interaction with helix 1

were occupied by Val and Trp, and position 53 by the highly conserved Arg which binds to the sugar-phosphate backbone of DNA.

An alignment of the regions lying N- or C-terminal of the HD furthermore showed that, despite little overall sequence identity, there were a number of amino acids maintained between OTEX and the other PEPP proteins (not shown). No significant homology was found with any other protein in the databases.

	Helix 1	Helix 2	Helix 3	Id	Pos
	10 20	30 >< 40	>< 50 60		
HsOTEX	**PRTRRTKFTL LQVEELESVF**	**RHTQYPDVPT RRELAENLGV**	**TEDKVRVWFK NKRARCRRHQ**	**100**	**Xq24**
AmPaxD	Q-RS-----H A-LNA--KA-	QK------Y- -E---HR-SL	--AR-Q---S -R---L-KKD	55	
HsESXR1	**K-R---A--Q F-LQ---NF-**	**DES-----VA -ER--AR-NL**	**---R-Q---Q -R--KWK-N-**	**53.3**	**Xq22**
HsARX	Q-RY--T--S Y-L----RA-	QK-H----F- -E---MR-DL	--AR-Q---Q -R--KW-KRE	53.3	Xp22.13
DmGsb-n	Q-RS--T--A E-L-A--RA-	SR------Y- -E---QTTAL	--ARIQ---S -R---L-K-S	53.3	2 60F1
HsPAX3	Q-RS--T--A E-L----RA-	ER-H---IY- -E---QRAKL	--AR-Q---S -R---W-KQA	51.7	2q35
HsPAX7	Q-RS--T--A E-L----KA-	ER-H---IY- -E---QRTKL	--AR-Q---S -R---W-KQA	51.7	1p36
HsCRX	Q-RE--T--R S-L----AL-	AK------YA -E-V-LKINL	P-SR-Q---- -R--K--QQR	51.7	19q13
DmGsb	Q-RS--T-SN D-IDA--RI-	AR------Y- -E---QST-L	--AR-Q---S -R---L-KQL	51.7	2 60F1
DmAl	Q-RY--T--S F-L----KA-	SR-H----F- -E---MKI-L	--ARIQ---Q -R--KW-KQE	51.7	2 21C1
HsARIX	Q-RI--T--S A-LK---R--	AE-H---IY- -E---LKIDL	--AR-Q---Q -R--KF-KQE	50	11q13
HsALX4	K-RN--T--S Y-L----K--	QK-H----YA -EQ--MRTDL	--AR-Q---Q -R--KW-KRV	50	11p11.2
HsSHOX	Q-RS--N--- E-LN---RL-	DE-H---AFM -E--SQR--L	S-AR-Q---Q -R--K--KQE	50	Xp22.32
MmEsx1	**--RY-IC--P I-LQ---AF-**	**QRV----LFA -V---RR--L**	**P-PR-Q---Q -R--KW--LR**	**50**	**X 57**
HsALX3	K-RN--T-ST F-L----K--	QK-H----YA -EQ--LRTDL	--AR-Q---Q -R--KW-KRE	48.3	1p21-p13
DmPrd	Q-RC--T-SA S-LD---RA-	ER-----IY- -E---QRTNL	--ARIQ---S -R---L-KQH	48.3	2 33C1
HsTHG1	**QQPNVHA--P --LQ---RI-**	**QRE-F-SEFL --R--RSMN-**	**--LA-QI--E -R--KW----**	**45**	**Xq24**
MmPsx2	**Q-----R--H S-LRD-GRL-**	**QENRF-SLRV --D--RWM--**	**D-SD-QE--- MR--LF---S**	**45**	**X 12.7**
MmPsx1	**L-Y---R--H S-LHD--RL-**	**QE-R--SLRA --D--RWM--**	**D-CD-QN--R MR--LFQ-NR**	**43.3**	**X 12.7**
MmEhox	**Q-SLHYN-QW W-LQ---RI-**	**QQNHFIRAEE --H--RWI--**	**S-AR-MT--- KR-EHF--G-**	**36.7**	**X A2**
MmRIKEN	**RHGWQQS-NV --LQ----I-**	**QCNH-ISTKE ANR--RSM--**	**S-AT-QE--L KR-EKY-SYK**	**31.7**	**Xq9D4Y3**
MmPem	**MPLQGSR-AQ HRLR----IL**	**QR-NSF--- -ED-DRLMDA**	**CVSR-QN--- IR--AA--TR**	**31.7**	**X 12.7**
RnPem	**MPL--PGS-Q RRLA---RIL**	**LSSGSSSG-- WE--DRWMDI**	**SVSR-QN--- IR--AY--NR**	**30**	**Xq35-36**

Figure 21: Amino acid sequence alignment of HDs from OTEX and related proteins. *Members of the PEPP subfamily are underlined and in bold. Dashes indicate identity with human OTEX sequence. The percentage identity (Id) as well as the chromosomal localization (Pos) are given in the right-hand columns.*

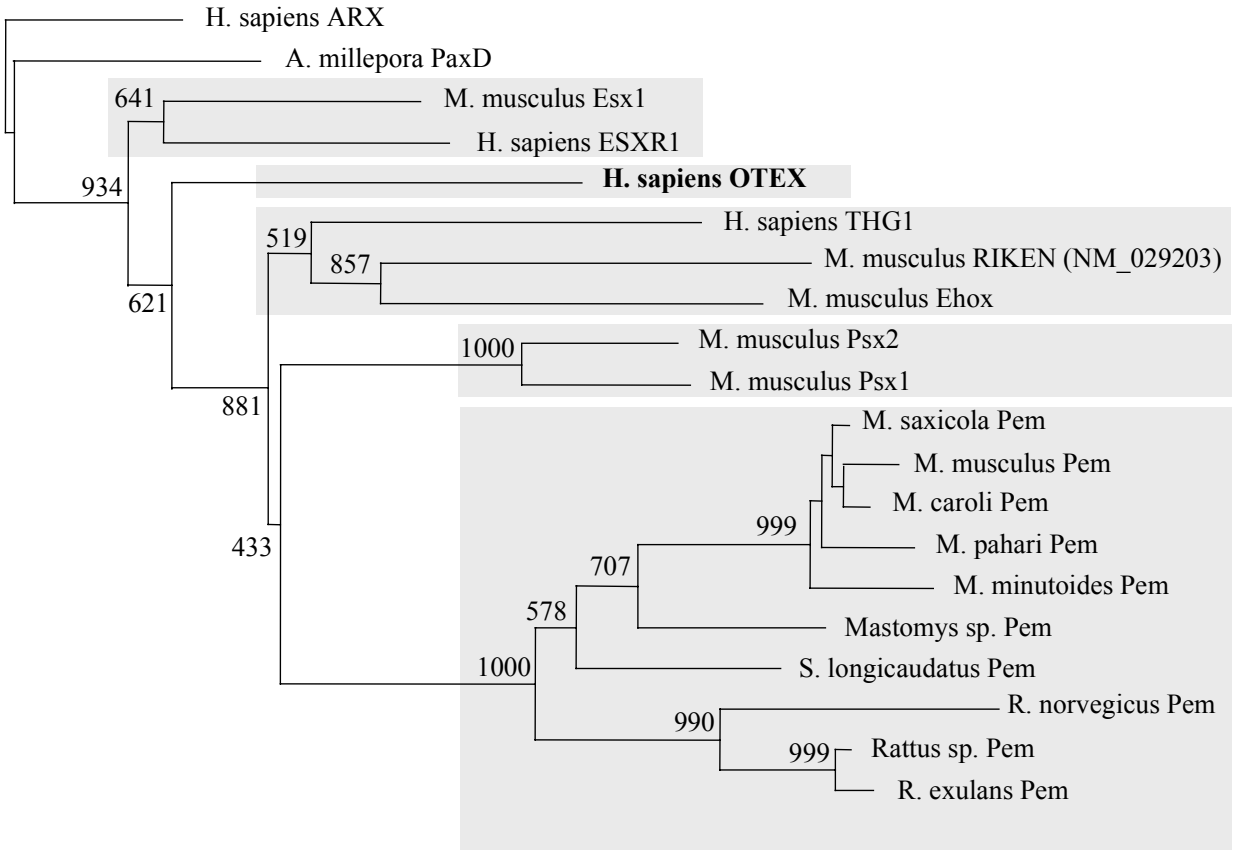

Figure 22: Phylogenetic analysis of PEPP HD sequences. *The tree is shown as a rooted phylogram using human ARX as outgroup. The five subgroups of the PEPP family are shaded in grey. The numbers near the branching nodes indicate the bootstrap values. For clarity, some bootstrap values were omitted.*

2.2.3. Chromosomal localization and organization of the OTEX gene

A search in human genome databases allowed to map the *OTEX* gene to chromosome X, at position Xq24. All the other *PEPP* genes are also found on chromosome X. The organization of the *OTEX* gene was established by comparing the cDNA and genomic sequences. The *OTEX* gene was found to be composed of three exons and two introns (Figure 23 A). The first exon comprised the 5´ untranslated region and more than half of the coding part. The second exon coded for the central part of the HD, and the third one for the remainder of the protein and the complete 3´ untranslated region. Both introns started with GT and ended with AG (Figure 23 B), in accord with the splicing rules (Breathnach et al., 1981). They interrupted codons at different positions and were therefore not in the same phase.

A comparison with other *PEPP* genes showed striking similarities. The intron interrupting the HD coding sequence after position 46 is found in *Pem*, *Esx1*, *ESXR1*,

Psx2 and *THG1*, and has also been reported in other homeobox genes. The intron found in *OTEX* after the codon for HD position 31 is far more unusual but also present in other *PEPP* genes as well as in *aristaless* (Galliot et al., 1999). Other *PEPP* subfamily members possess one or more additional 5´ exons but an analysis of the *OTEX* upstream genomic sequence using a prediction program did not reveal the presence of putative exons.

A

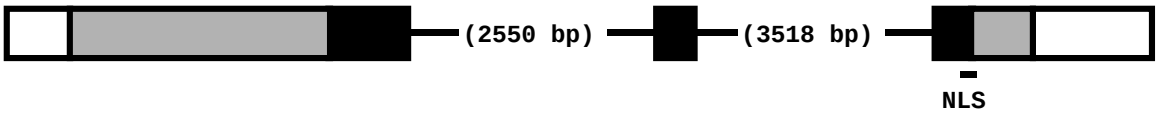

B

intron	EXON	intron	Phase
AACTA..	(473 bp) ..ACAAGgtaagtgg	(2550 bp)	2
ctccacagAAGGG..	(46 bp) ..TGCGGgtcagtac	(3518 bp)	0
gattgtagGTTTG..	(236 bp) ..TAAAG		

Figure 23: Gene structure of OTEX. *(**A**) Schematical representation of the OTEX gene. The 5´ and 3´ untranslated ends are in white, the coding region is in grey or black (for the HD). Approximate location of the NLS is indicated. (**B**) The sequence of the exon/intron boundaries is given. The phase indicates after which position of the codon the intron is located.*

2.2.4. Analysis of the putative OTEX promoter

The region upstream of the *OTEX* start codon up to position –278 was analyzed in order to identify consensus SREs. However no such elements were found (Figure 24). Therefore it was looked for the response element half-sites TGTTCT and AGAACA and the latter was found starting at position –83 (Figure 24). No sequence resembling the other half-sites could be identified in the vicinity. Several, more degenerated half-sites could be found in other regions of the *OTEX* promoter (not shown). A potential cap site motif with the consensus Py-Py-C-A-Py-Py-Py-Py-Py was located about 30 bp upstream of the 5´ end of the longest clone isolated (see also Figure 20) (Xu et al., 1991). There was no sequence resembling the TATA

consensus at the appropriate upstream position but several Py-Py-A_{+1}-N-T/A-Py-Py initiator consensus motifs (Lo et al., 1996) (Figure 24). The absence of a *bona fide* TATA box has already been reported for the rat and mouse *Pem* proximal promoters (Maiti et al., 1996a; Barbulescu et al., 2001).

-278 ccccaccctc cacccacacc cccatcccca cctgcacccc accccacact

-228 cacaaccccc cactcccacc tgcaacaccc ccactcccca cccgcacccc

-178 ccaacttccc atccccccac tcctctccat tccctctctt gcttgtgcgc

-128 ataagcaagt cccactcatt gcaactgtaa ccaataccaa gcatga**g**aa**c**

-78 aggaactagc *tccaccctc*t aacccccact ccagctgcag acgccacgga

-28 gtttgtgcag gggcgcagcg ctccagcc ATG

+1

Figure 24: Nucleotide sequence of the putative OTEX promoter. *The upstream region 5' of the first OTEX exon is shown. Numbering starts at the translation initiation codon, given in uppercase letters. A half-site with the consensus AGAACA is underlined. The C and G contact bases with which the AR is thought to interact are in bold. The sequence resembling an initiator motif with the consensus Py-Py-A_{+1}-N-T/A-Py best is boxed. A potential cap site motif with the consensus Py-Py-C-A-Py-Py-Py-Py-Py is given in italics.*

2.2.5. Tissue distribution of OTEX transcripts

To analyze in which tissues *OTEX* RNA was expressed, RT-PCR was performed on reverse-transcribed human RNA using specific oligonucleotides. Primers overlapping the initiation or stop codons were used in order to assess the expression levels of full-length *OTEX* transcripts only. This also excluded the risk of amplifying contaminating genomic DNA as two introns were present in the corresponding gene region. The strongest signal was detected in the ovary, testis and epididymis, hence the name OTEX (Figure 25). Specific transcripts were additionally detected in the prostate and the mammary gland. A very weak expression was visible in the uterus. Expression in the main steroid target tissues is another feature shared by *OTEX* with the other *PEPP* family members.

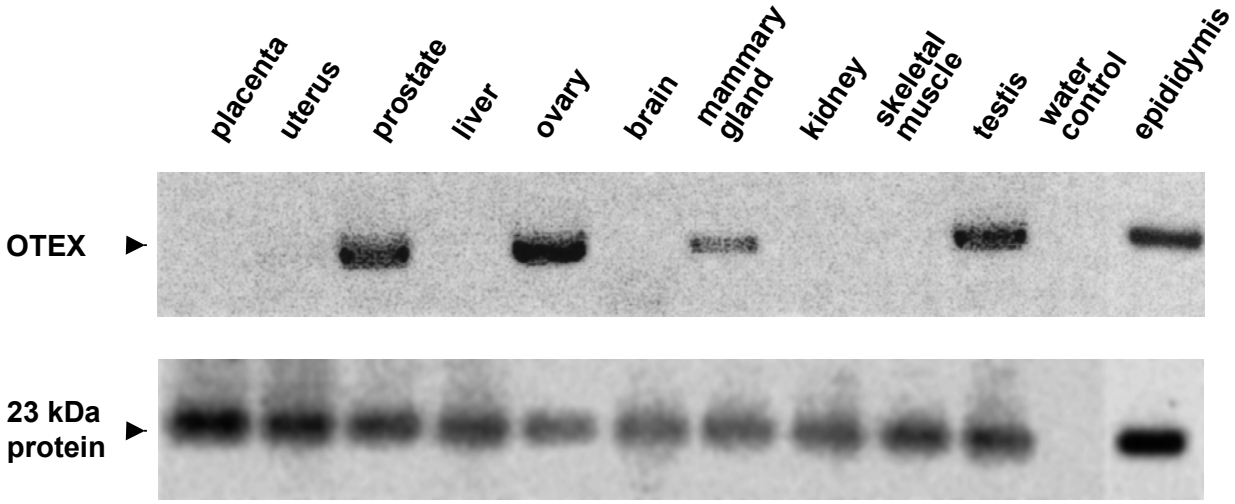

Figure 25: Tissue distribution of OTEX. *RT-PCR was performed with OTEX-specific primers using reverse-transcribed human RNA from the indicated organs. The PCR products were separated on gel and stained with ethidium bromide. The RNA levels of the 23 kDa highly basic protein were determined as control.*

2.2.6. Androgen regulation of OTEX

Expression of *Pem*, the founding member of the *PEPP* family is strongly regulated by androgens in the testis and epididymis (Maiti et al., 2001). *OTEX* transcripts are found in the testis, epididymis and prostate, three main target organs of androgens. Therefore PC-3 cells (which do not express the AR) and PC-3/ARwt cells, a derived line stably transfected with the human wild-type androgen receptor were examined for *OTEX* expression. RNA was extracted and analyzed by RT-PCR using primers that amplified the full coding sequence of *OTEX* (Figure 26). The results showed that *OTEX* was not expressed in the parental PC-3 cell line whereas a specific signal was generated from RNA originating from the PC-3/ARwt cells. This signal was much amplified if the PC-3/ARwt cells were treated beforehand with the androgen R1881, indicating that expression of the *OTEX* gene was controlled by androgen.

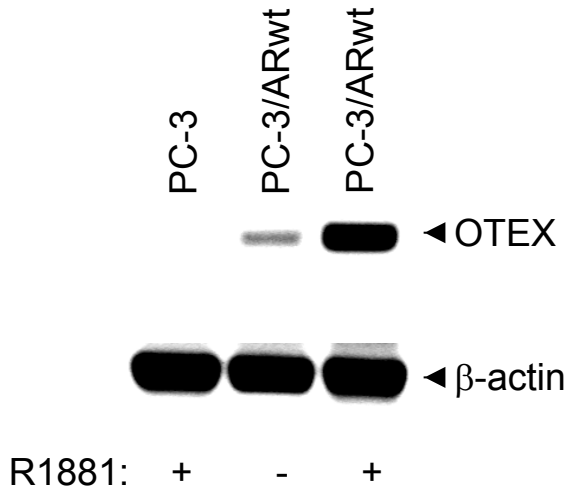

Figure 26: Androgen regulation of OTEX expression. *RT-PCR was performed with OTEX-specific primers using reverse-transcribed RNA extracted from the cell lines indicated. The PCR products were separated on gel and stained with ethidium bromide. The RNA levels of β-actin were determined as control.*

2.2.7. Subcellular localization of OTEX and identification of the NLS

As *OTEX* potentially coded for a homeobox transcription factor it was interesting to determine the subcellular localization of the corresponding protein. Full-length *OTEX* coding sequence was fused to a myc tag sequence in the pcDNA plasmid. Transfection was performed using CV-1 or PC-3 cells, and the results were visualized by fluorescence microscopy. An anti-myc antibody and a secondary rhodamine-labelled antibody were used to detect the OTEX-myc fusion protein in CV-1 cells. For PC-3 cells, a cyanine-labelled secondary antibody was used. DAPI staining was performed in parallel to localize the cell nuclei. The results showed that in both CV-1 and PC-3 cells, OTEX was localized exclusively in the nucleus (Figure 27).

Active nuclear translocation usually necessitates the presence of a NLS recognized by a receptor named importin (Jans et al., 2000). In order to identify this signal, a stretch of the OTEX protein that contained several Arg and Lys residues was mutated, as these positively charged amino acids are known to form the core of different NLS (Boulikas et al., 1994). Two mutants of the same region were generated, one with a modified 18-amino acid stretch (positions 147 to 164: mutant 1; Figure 20) and the other with a modified 10-amino acid stretch (positions 155 to 164: mutant 2; Figure 20 in bold; Figure 27). Expression vectors for mutated OTEX were transfected into PC-3 and CV-1 cells and after 24h cells were immunostained. Both mutants were mainly localized in the cytoplasm with only minor staining in the nucleus (Figure 27). The residual nuclear staining was probably due to passive diffusion into the nucleus facilitated by the comparatively small size of the OTEX-myc fusion protein. A comparison between the identified NLS of OTEX and the corresponding region of other PEPP proteins allowed us to infer the consensus motif RAxxRRxxRx (Table 3).

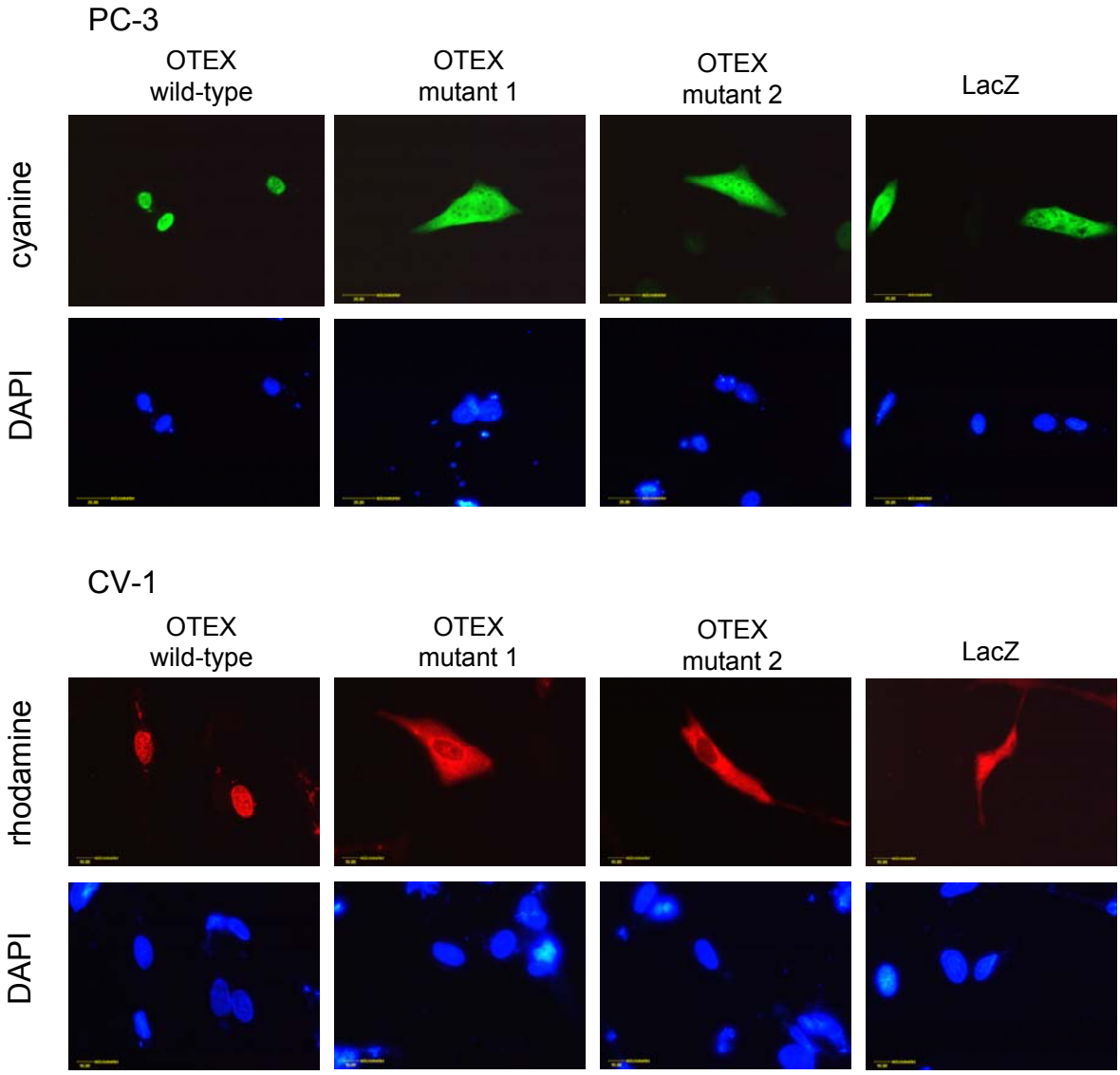

Figure 27: Nuclear localization of OTEX. *Cells were transfected with expression constructs for the indicated proteins. Subcellular localization was determined using a specific primary antibody and a fluorophore-labelled secondary antibody. DAPI staining was carried out to visualize the nuclei.*

Protein	NLS
HuOTEX	RARCRRHQRE
HuESXR1	--KWK-N-VL
HuTHG1	--KW-----A
MoPem	--AA--TR-R
MoEsx1	--KW--LR-A
MoPsx1	--LFQ-NR-V
MoPsx2	--LF---S-L
RtPem	--AY--NR-R
Consensus	RAxxrRxxrx

Table 3: Comparison of NLS sequences found in PEPP proteins. *The amino acid sequence of OTEX NLS was written out. In the other sequences, dashes indicate identity with OTEX. The consensus was defined as amino acids maintained in at least 6 out of 8 sequences.*

2.2.8. Activity of OTEX in one- and two-hybrid assays

In order to find out whether OTEX possessed an independent transactivation function, a one-hybrid assay was performed. The *OTEX* coding region was introduced into the pCMV-BD plasmid, in frame with the GAL4 DNA-binding domain. Following cotransfection of CV-1 cells with a vector containing GAL4 DNA elements upstream of a luciferase gene, reporter activity was measured. No stimulation of activity was detected with any of the plasmid concentrations tested, as compared to samples where only the reporter plasmid was transfected (Figure 28 A). Comparable results were observed using PC-3 cells (not shown).

Several homeobox proteins form homodimers or heterodimers for DNA binding. In order to find out whether OTEX interacted with itself, plasmids coding for fusions between OTEX and the GAL4 DNA-binding domain, or between OTEX and the NFκB activation domain were cotransfected with the reporter vector. No significant interaction between the OTEX fusion proteins could be evidenced in CV-1 cells (Figure 28 B) or in PC-3 cells (not shown).

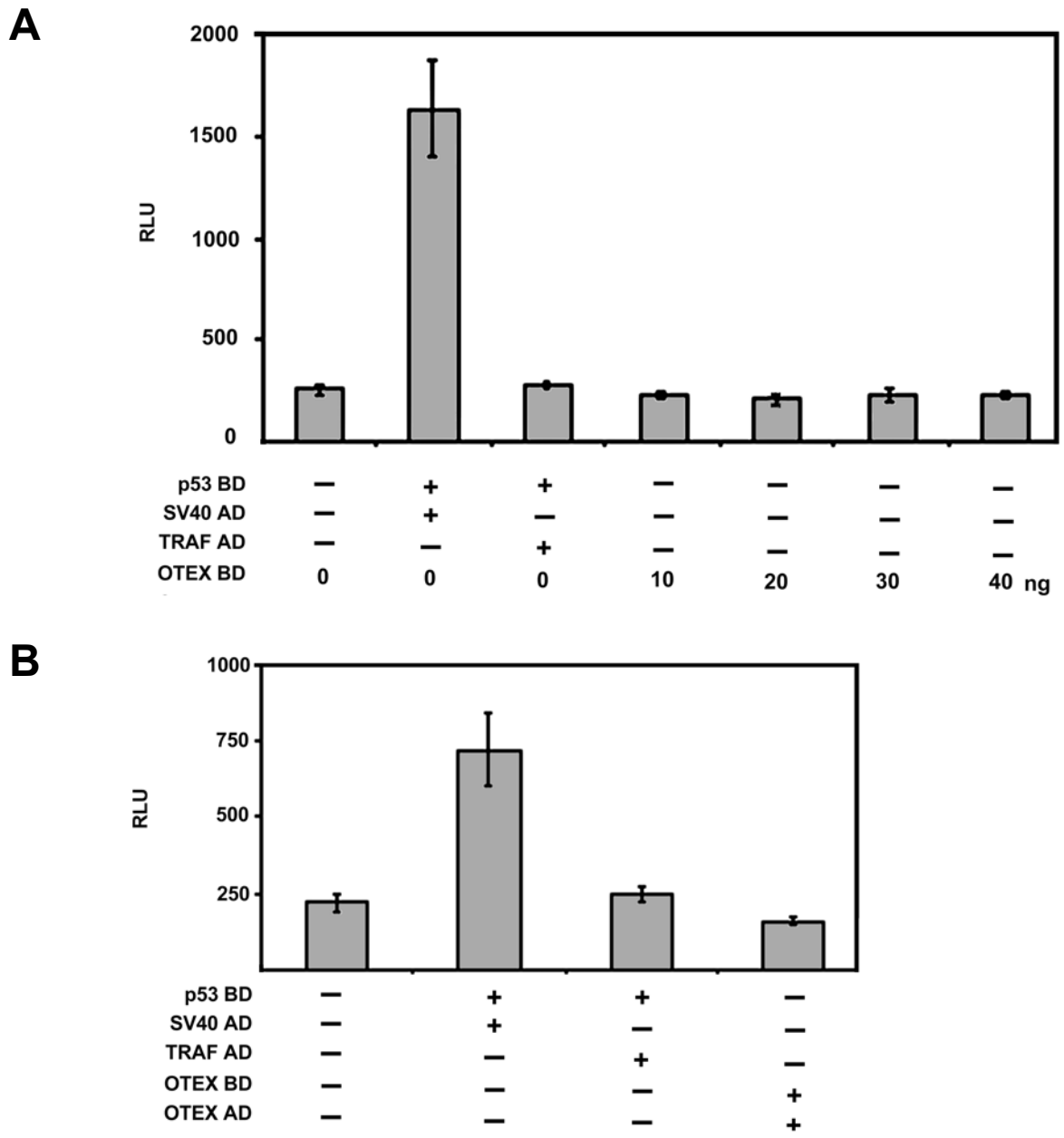

Figure 28: OTEX activity in one- and two-hybrid assays. *(A) CV-1 cells were transfected with the indicated amounts of an expression vector for OTEX fused to the DNA-binding domain of Gal4. (B) CV-1 cells were cotransfected with expression vectors for OTEX fused to the DNA-binding domain of Gal4 and OTEX fused to the transactivation domain of NFκB. The interaction between p53 and SV40 large T-antigen was determined as positive control. Transactivation was measured after 24 h as the induction of luciferase reporter activity in relative light units (RLU). The results are a representative of three separate experiments and the bars are the mean ±SEM of sextuplicate values.*

2.2.9. OTEX inhibits cell proliferation

Many homeobox proteins play important roles in differentiation. One characteristic of most differentiated cells is their low proliferation rate. Therefore the proliferation of CV-1 cells transiently transfected with an OTEX-expressing construct was analyzed. As controls the NLS mutants of OTEX or Lac-Z were expressed (Figure 29). The cellular ATP content was measured as index for the number of viable cells after one, two and three days. The cells overexpressing wild-type OTEX grew slowest. In presence of the NLS mutants of OTEX a stronger proliferation rate of the transfected cells was observed. The growth rate of cells transfected with a Lac-Z expression vector was the highest.

These results indicate that ectopic OTEX expression reduces the proliferation rate of CV-1 cells more than a predominantly cytoplasmic form does, in line with a role of OTEX as a homeobox transcription factor that might control genes involved in cellular differentiation.

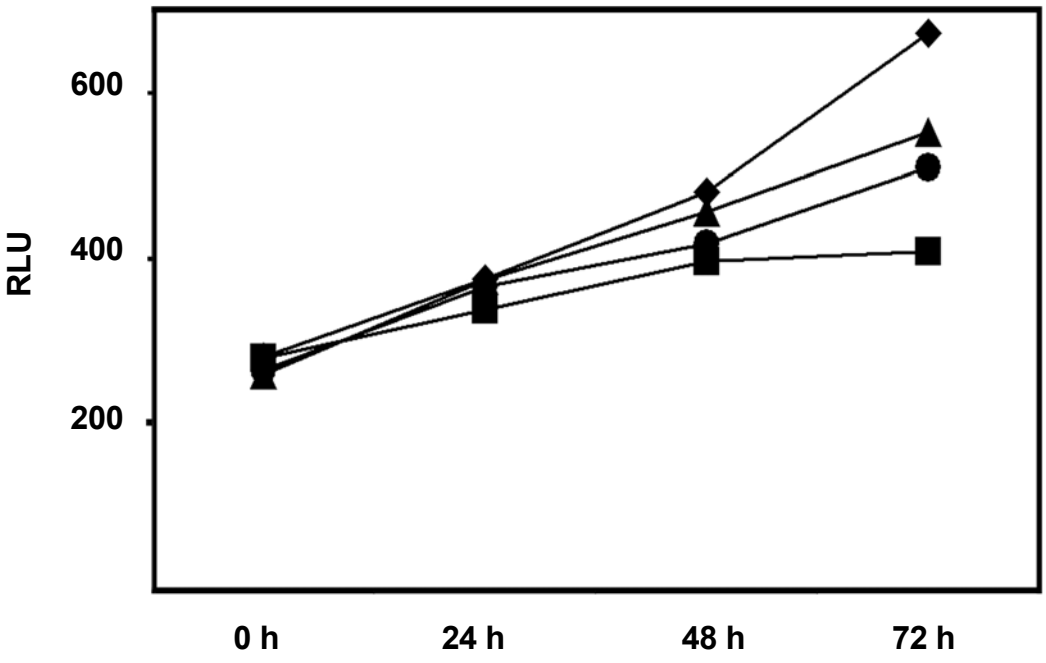

Figure 29: OTEX overexpression reduces CV-1 proliferation. *CV-1 cells were transiently transfected with expression plasmids for wild-type OTEX (squares), NLS mutation-1 of OTEX (circles), NLS mutation-2 of OTEX (triangles) or Lac-Z as a control (diamonds). The cell number was determined after one, two and three days using a light emitting assay in relative light units (RLU). The results are a representative of three separate experiments measured as sextuplicate values.*